The Astrophysical Journal Letters, 789:L13 (5pp), 2014 July 1 doi:10.1088/2041-8205/789/1/L13

RELICS OF GALAXY MERGING: OBSERVATIONAL PREDICTIONS FOR A WANDERING MASSIVE BLACK HOLE AND ACCOMPANYING STAR CLUSTER IN THE HALO OF M31

Toshihiro Kawaguchi[1,2], Yuriko Saito[3,4], Yohei Miki[2], and Masao Mori[2]
[1] Astronomy Data Center, National Astronomical Observatory of Japan, Mitaka, Tokyo 181-8588, Japan; ts.kawaguti@nao.ac.jp
[2] Center for Computational Sciences, University of Tsukuba, Tsukuba, Ibaraki 305-8577, Japan
[3] Department of Astronomical Science, The Graduate University for Advanced Studies (SOKENDAI), Mitaka, Tokyo 181-8588, Japan
[4] Subaru Telescope, National Astronomical Observatory of Japan, 650 North A'ohoku Place, Hilo, HI 96720, USA
Received 2014 January 16; accepted 2014 May 28; published 2014 June 17

ABSTRACT

Galaxies and massive black holes (BHs) presumably grow via galactic merging events and subsequent BH coalescence. As a case study, we investigate the merging event between the Andromeda galaxy (M31) and a satellite galaxy. We compute the expected observational appearance of the massive BH that was at the center of the satellite galaxy prior to the merger and is currently wandering in the M31 halo. We demonstrate that a radiatively inefficient accretion flow with a bolometric luminosity of a few tens of solar luminosities develops when Hoyle–Lyttleton accretion onto the BH is assumed. We compute the associated broadband spectrum and show that the radio band (observable with EVLA, ALMA, and the Square Kilometre Array) is the best frequency range in which to detect the emission. We also evaluate the mass and the luminosity of the stars bound by the wandering BH and find that such a star cluster is sufficiently luminous that it could correspond to one of the star clusters found by the PAndAS survey. The discovery of a relic massive BH wandering in a galactic halo will provide a direct means of investigating in detail the coevolution of galaxies and BHs. It also means a new population of BHs (off-center massive BHs) and offers targets for clean BH imaging that avoid strong interstellar scattering in the centers of galaxies.

Key words: accretion, accretion disks – black hole physics – galaxies: dwarf – galaxies: individual (M31) – galaxies: interactions – galaxies: star clusters: general

1. INTRODUCTION

In the hierarchical structure formation scenario in a cold dark matter universe, dark matter halos and their galaxies have grown and built up their mass by colliding and merging with ambient sub-halos and satellite galaxies (e.g., Bullock & Johnston 2005; Chiba et al. 2005). Furthermore, massive galaxies harbor central massive black holes (BHs) whose masses ($M_{\rm BH}$) are correlated with the mass of the spheroidal component of the host galaxy (Kormendy & Richstone 1995). Currently, the BH–bulge relation is observed down to $M_{\rm BH}$ of $\sim 10^5\ M_\odot$ (Barth et al. 2005; Xiao et al. 2011). One is therefore naturally led to believe that a massive BH also increases its mass after a galaxy collision by merging with the BH that was located at the center of a satellite galaxy, as presumed in semi-analytical calculations for the galaxy and BH evolution (Kauffmann & Haehnelt 2000).

There is, however, no clear observational evidence that the merging events between galaxies really lead to the merging of massive BHs. The central BH of a satellite galaxy likely wanders in the halo of its host galaxy after a galaxy merging event, before it finally sinks toward the center of the host galaxy due to the dynamical friction (Bellovary et al. 2010). Namely, the massive BH is expected to be located far away from the galactic center.

There are some known implications for the BH growth associated with merging events. For instance, NGC 6240 (at $\sim$100 Mpc) is an irregular starburst galaxy, indicative of a recent galaxy merging event, and harbors two massive BHs with a projected separation of 1 kpc (Komossa et al. 2003). Double or triple massive BHs in a colliding galaxy are now commonly found (e.g., Koss et al. 2011). Moreover, ESO 243–49, an edge-on disk galaxy at a similar distance, shows a bright X-ray point source (hyper-luminous X-ray source) at a projected distance from the center of 3.5 kpc (Farrell et al. 2009). A detailed X-ray spectral analysis revealed a $\sim 2\times10^4\ M_\odot$ BH (Godet et al. 2012). Although this intermediate-mass BH candidate may have been the central BH of a satellite galaxy (Farrell et al. 2012), there is no clear evidence for a merging event in this galaxy. In the case of some massive binary BH candidates (Sudou et al. 2003; Boroson & Lauer 2009), their large distances make it difficult to detect merging signatures.

As a case study, we focus on the nearby galaxy M31 (Andromeda galaxy). Its proximity to the Galaxy, at a distance of 780 kpc (McConnachie et al. 2003; $1'' \approx 4$ pc and $1^\circ \approx 14$ kpc), allows detailed investigations into the faint stellar structures, showing that M31 is evidently in the process of the galaxy collision (Ibata et al. 2001; Irwin et al. 2005; Fardal et al. 2007; Mori & Rich 2008). Thus, it is a unique laboratory in which to examine how galaxy evolution and BH growth take place. Another advantage is the detectability: M31's proximity is essential in order to detect the faint a low-luminous emission of a wandering BH.

Some stellar substructures in the M31 halo were shown to be remnants of a minor merger about 1 Gyr ago. In a previous paper (Miki et al. 2014, hereafter Paper I), we established the probable position of the associated wandering massive BH by performing *N*-body simulations. Finding this BH will provide us with clues for understanding the coevolution of galaxies and massive BHs. If we really discover a massive BH wandering in a galactic halo, it indicates that many such wandering BHs, the remnants of satellite galaxies, in distant galaxies are missing due solely to sensitivity limits of current instruments. Since all massive BHs have thus far been found at the center of each galaxy, it opens up the possibility for the discovery of a new population of massive BHs.

In this Letter, we determine the most efficient waveband(s) to detect a wandering massive BH of the satellite galaxy in the M31 halo. In the next section, the basic properties of the satellite galaxy and its central BH are briefly described. Then,

we present the expected emission from the wandering BH and from an assembly of stars bound by the BH. We conclude with a summary and discussion of this study in Section 4.

2. THE COLLIDING SATELLITE GALAXY AND ITS CENTRAL MASSIVE BLACK HOLE

We briefly summarize the basic properties of the satellite galaxy that is interacting with M31.

As the satellite dwarf galaxy falls toward M31, it is elongated by the tidal force from M31, and eventually destroyed following a series of pericentric passages. Now, we see only the remnants of the satellite galaxy as a stellar stream (the so-called Andromeda stream) and two (western and northeastern) stellar shells (e.g., Ibata et al. 2001; Irwin et al. 2005). Detailed comparisons between observations and numerical simulations of the morphologies and the radial velocities of the stream and shells constrain the orbit, the mass and the concentration parameter of the satellite galaxy (Fardal et al. 2007; Mori & Rich 2008; Paper I).

Via the metallicity–mass relation of dwarf galaxies, the lower limit on the stellar mass of the progenitor is known to be $5 \times 10^8\,M_\odot$ (e.g., Mori & Rich 2008). An upper limit on the dynamical mass of the progenitor ($\leqslant 5 \times 10^9\,M_\odot$) comes from the disk thickness of M31 (Mori & Rich 2008).

The BH–bulge mass relation suggests that the progenitor dwarf galaxy has a massive BH with $M_{\rm BH}$ of about 1/500 of the mass of its host spheroidal component (Magorrian et al. 1998; Marconi & Hunt 2003). This raises the question of whether the colliding satellite galaxy did indeed have a central BH. Font et al. (2006) estimated the luminosity of the colliding galaxy to be $M_B \approx -17$ mag ($L_B \approx 10^9\,L_\odot$). Adopting the B–I colors of elliptical and spiral galaxies (Fukugita et al. 1995), this corresponds to M_I of -19.3 and -18.7 mag, respectively. Galaxies around the current low-mass end in the BH–bulge mass relation are of similar or even fainter luminosities. For example, POX 52, a galaxy harboring a $\sim 10^5\,M_\odot$ BH, has a dwarf elliptical morphology with $M_I = -18.4$ mag (Thornton et al. 2008). Host galaxies of $10^{5-6}\,M_\odot$ BHs have $-23 < M_I < -18.8$ mag (Jiang et al. 2011). Thus, we suspect that the colliding satellite galaxy had a massive BH at its center with $M_{\rm BH}$ of (at most) about $10^7\,M_\odot$ (i.e., 1/500 of $5 \times 10^9\,M_\odot$). We describe the $M_{\rm BH}$-dependency of the results later.

If there was a central massive BH in the satellite galaxy, then where is the BH now? Based on the N-body simulations in Paper I, which involved an intensive survey of parameters relevant to the collision followed up by high-resolution calculations, we identified five orbit models that reproduce the stream and the two shells well. The current position of the BH is then constrained to a small region ($\sim 0.^\circ 6 \times 0.^\circ 7$) in the eastern outskirts of the M31 disk. The expected proper motion is 33–43 μas yr^{-1}. The distance of the BH from the center of M31 is 18–49 kpc, with a projected distance on the sky plane of 0.4–0.8 deg.

3. SEARCHING FOR THE WANDERING BH

We now focus on the emission from the wandering massive BH and trailing stars.

3.1. Hoyle–Lyttleton–Bondi Accretion onto the BH

First, we estimate the accretion rate onto the wandering massive BH. Such a BH, moving with a velocity v, will capture the surrounding interstellar medium (ISM) of density ρ and sound speed c_s via Hoyle–Lyttleton–Bondi accretion at a rate $\dot{M}$ (Hoyle & Lyttleton 1939; Bondi & Hoyle 1944):

$$\dot{M} = 4\pi G^2 \frac{\rho M_{\rm BH}^2}{\left(v^2 + c_s^2\right)^{1.5}}. \quad (1)$$

We assume that the ISM has the same density profile as the mass profile of M31, namely, a Hernquist bulge, an exponential disk, and a Navarro–Frenk–White halo (e.g., Fardal et al. 2007). A constant gas fraction (with respect to the total mass of dark matter+star+gas) of 0.1 is adopted. For the sound speed, we assume an ISM temperature of 10^4 K for the disk and bulge gas, and of 10^6 K for the halo gas.

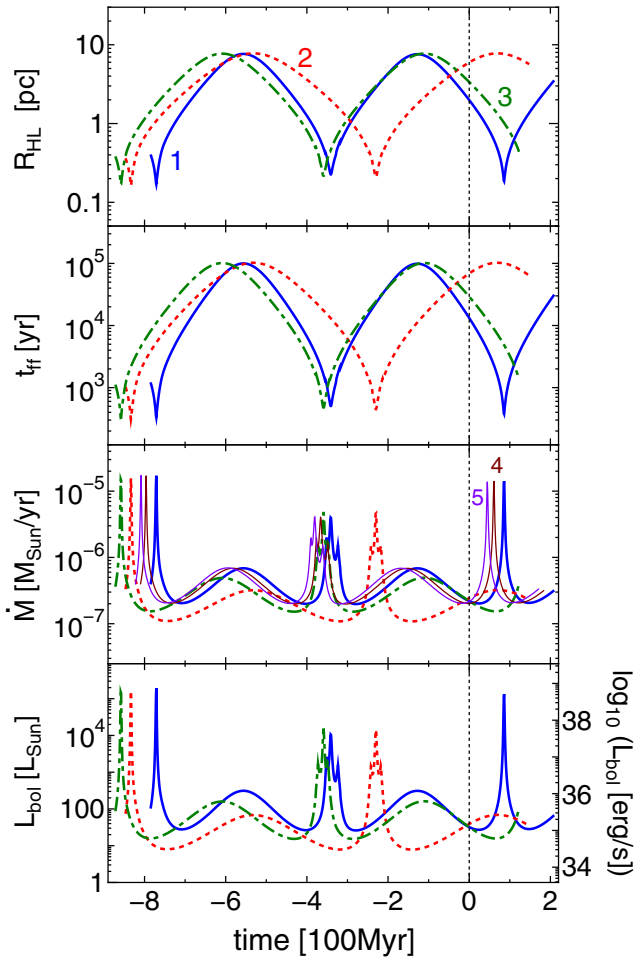

Figure 1. Time variation of the Hoyle–Lyttleton radius $R_{\rm HL}$, the free-fall timescale at $R_{\rm HL}$, the accretion rate $\dot{M}$, and the bolometric luminosity for $M_{\rm BH} = 10^7\,M_\odot$. Blue solid, red dashed, and green dot-dashed lines indicate the successful orbit models with ID 1-3 in Paper I. For $\dot{M}$, we also plot the results for ID 4 and 5 with thin solid lines in brown and purple, respectively. For different BH masses, $R_{\rm HL} \propto M_{\rm BH}$, $t_{\rm ff} \propto M_{\rm BH}$, $\dot{M} \propto M_{\rm BH}^2$ and $L_{\rm bol} \propto M_{\rm BH}^3$. The vertical dotted line indicates the present time.

The upper three panels of Figure 1 show the Hoyle–Lyttleton radius $R_{\rm HL}$ [$\equiv 2GM_{\rm BH}/(v^2 + c_s^2)$], the free-fall timescale at that radius ($R_{\rm HL}^{1.5}/\sqrt{GM_{\rm BH}}$), and $\dot{M}$. Among the five orbit models that reproduce the stellar structures of M31, the representative three cases (with ID 1, 2, and 3) are shown in all the panels for a BH mass of $10^7\,M_\odot$. Since the remaining two cases (ID 4 and 5) show time variations similar to ID 1, their results are shown only in the third panel by thin solid lines. To take into account different BH masses, each curve can be scaled as, $R_{\rm HL} \propto M_{\rm BH}$, $t_{\rm ff} \propto M_{\rm BH}$ and $\dot{M} \propto M_{\rm BH}^2$. The time coordinate is shown with

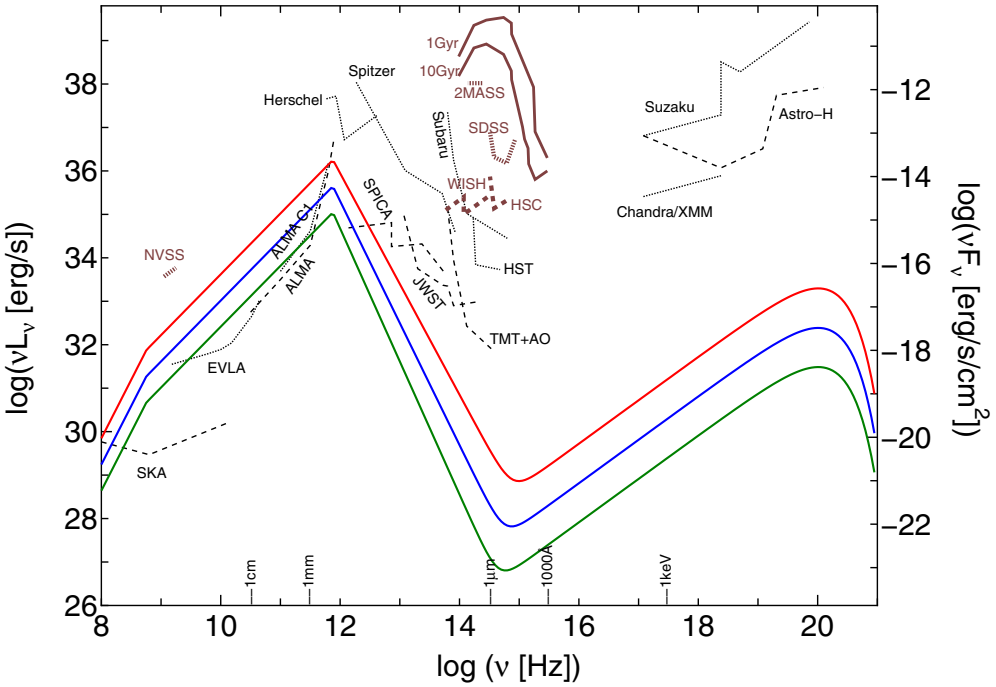

Figure 2. Expected spectral energy distribution of the wandering BH (solid curves) for three different BH masses (5×10^6 (green), 10^7 (blue), and $2 \times 10^7\,M_\odot$ (red), with $L_{\rm bol}$ of 4, 32, and $260\,L_\odot$, from the bottom to the top, respectively). The right axis corresponds to the flux at the distance of M31. Black dotted and dashed lines indicate the detection limits (10σ in 10^4 s integration) of the existing and planned facilities, respectively. The emission from the accretion flow is detectable only in the radio band (frequency less than 10^{12} Hz). Brown, thick solid curves are spectra of a star cluster that are 1 Gyr and 10 Gyr old. Brown, thick dotted and dashed lines indicate the 10σ sensitivities of wide-field surveys.

respect to the present time, so that negative values indicate the past, and vice versa.

Around the pericenters (e.g., at −770, −340 and +86 Myr for ID 1), $R_{\rm HL}$ decreases due to the large BH velocity, whereas it has maxima around the apocenters (at −560 and −130 Myr for ID 1). There are two types of peaks in the time variation of $\dot{M}$. At the pericenters, the high values of $\dot{M}$ are due to the high ISM density near the M31 center, lasting only a relatively short time because of the large BH velocity. On the other hand, broad peaks in $\dot{M}$ around the apocenters are caused by small BH velocities.

To be precise, the estimated $\dot{M}$ is the mass capturing rate, which does not necessarily equal the mass accretion rate onto the BH. We now evaluate the outer radius of the accretion disk/flow, which is determined by the angular momentum of the captured ISM. At the apocenter, $R_{\rm HL}$ is largest at about 10 pc, i.e., 10^7 Schwarzschild radii ($R_{\rm Sch}$) for a $10^7\,M_\odot$ BH. The ISM kinematics is mostly isotropic, but has a tiny anisotropy which forms the accretion disk. An ISM captured at that distance from the BH will have a specific angular momentum of about 5 km s^{-1} pc (Phillips 1999). This corresponds to the Keplerian angular momentum at $\sim 500 R_{\rm Sch}$ for a $10^7\,M_\odot$ BH. Due to the redistribution of the angular momentum within the flow, the disk is a few times larger than the angular momentum barrier (e.g., Machida et al. 2004). Thus, we hereafter assume the size of the accretion flow to be $1000 R_{\rm Sch}$. Therefore, the accretion timescale within the flow (∼ the free-fall timescale from the outermost radius divided by the viscosity parameter; Narayan & Yi 1995) is negligible compared with that from $R_{\rm HL}$ to the outermost radius of the flow. It follows that the time required for the captured gas to reach the BH is largely governed by the free-fall timescale at $R_{\rm HL}$, which is $\sim 10^5$ yr at most (Figure 1), and is small compared to the orbital timescale of the wandering BH (some 10^8 yr).

The expected $\dot{M}$ is much smaller than the Eddington rate ($\sim 10\,L_{\rm Edd}/c^2 \approx 0.2\,M_\odot$ yr^{-1} for a $10^7\,M_\odot$ BH) by several orders of magnitude. We therefore adopt an accretion model for such low rates, the advection-dominated accretion flow (ADAF) model. By imposing a radiative efficiency (the conversion efficiency from the rest mass energy of the infalling gas to the emergent radiation) of $\dot{M}/(L_{\rm Edd}/c^2)$ (Narayan & Yi 1995), we calculate the bolometric luminosity as a function of time (bottom panel of Figure 1). The bolometric luminosity is a few tens of $L_\odot$ at the present time, and at most $\sim 10^{(4-5)}\,L_\odot$ around the pericenters.

3.2. Radiation from the Accretion Flow

Based on the current value of $\dot{M}$ shown in Figure 1, we present the expected broadband spectral energy distribution of the accretion flow in Figure 2, using a simplified ADAF model (Mahadevan 1997). Since the five successful orbit models exhibit almost the same $\dot{M}$, we only show the case for ID 1. Below $\sim 10^{12}$ Hz, self-absorbed synchrotron emission emerges. The outermost radius ($10^3\,R_{\rm Sch}$) contributes at $\sim 10^{8.7}$ Hz, while the innermost region at $3\,R_{\rm Sch}$ has a peak at $\sim 10^{12}$ Hz. Above that frequency, inverse Compton scattering of the radio seed photons arises up to 1 μm. Bremsstrahlung emission appears at higher frequencies.

The detection limits (10σ in 10^4 s integration; based on, e.g., Perley et al. 2011 for EVLA and the ALMA sensitivity Calculator[5]) of various instruments for a point source are shown by solid and dotted lines in black. The size of the accretion flow is about 10^{-3} pc ($10^3\,R_{\rm Sch}$ for a $10^7\,M_\odot$ BH), corresponding to 0.3 mas. Thus, the flow is practically a point source for those facilities.

[5] http://almascience.nao.ac.jp/documents-and-tools

Because the emission from the BH is detectable only at frequencies less than 10^{12} Hz, radio observations with EVLA, ALMA, and the Square Kilometre Array (SKA) are crucial to finding the wandering BH (see also Strader et al. 2012). Since the luminosity from the self-absorbed synchrotron emission scales as $\propto M_{\rm BH}^{2/5}\dot{M}^{4/5} \propto M_{\rm BH}^{2}$ (Mahadevan 1997), the minimum detectable BH mass $\approx 3 \times 10^5\,M_\odot$ for SKA. If the accretion rate is much smaller than that in Equation (1) by, e.g., 2.5 dex, as is suggested by Perna et al. (2003) and Bower et al. (2003), the minimum detectable BH mass increases to about $3 \times 10^6\,M_\odot$. Winds from stars surrounding the BH (Section 3.3) could increase the accretion rate and thereby the luminosity of the flow. Radio flares, as seen in Sgr A* (Miyazaki et al. 2004), will make the detection even easier. The radio source 37W207 (Walterbos et al. 1985), located within our predicted region, may actually be the wandering BH.

3.3. Star Cluster

The wandering BH likely trails stars that resided in the central region of the satellite galaxy (see O'Leary & Loeb 2009 and Merritt et al. 2009 for star clusters surrounding recoiled BHs). The Hill radius $R_{\rm Hill}$ at the pericentric passage (with the minimum distance R_0 between the satellite and the M31 centers of 1.1 kpc) determines how many stars are still bound to the BH. The M31 bulge (with a mass $M_{\rm bulge}$ of $3 \times 10^{10}\,M_\odot$ and a scale length a of 0.6 kpc) will straggle stars outside $R_{\rm Hill}$ from the BH via the tidal force, where

$$R_{\rm Hill} = \left(\frac{M_{\rm BH}}{3\,M_{\rm bulge}}\right)^{\frac{1}{3}} R_0 \left(1+\frac{a}{R_0}\right)^{\frac{2}{3}} \quad (2)$$

$$\approx 70\,{\rm pc}\left(\frac{M_{\rm BH}}{10^7\,M_\odot}\right)^{\frac{1}{3}}. \quad (3)$$

The mass of stars in the satellite galaxy within this radius (≈18 arcsec), if distributed in a King profile (see Paper I for more details), amounts to about 10% of the BH mass of the satellite galaxy. If the presence of the central BH enhances the nuclear stellar density compared to that predicted by the King profile, the expected mass and luminosity of the star cluster will be higher, leading to an even easier detection.

Next, we utilize the stellar synthesis model PEGASE (Fioc & Rocca-Volmerange 1997) to calculate the spectra of an ensemble of stars for various ages after an instantaneous starburst (their Figure 1). In Figure 2, we draw such spectra for a star cluster of $10^6\,M_\odot$ in stellar mass and ages of 1 Gyr and 10 Gyr. The expected radiation is well above the 10σ sensitivities of near-infrared (IR) and optical, wide-field surveys, such as Sloan Digital Sky Survey, HyperSuprime-Cam, and WISH[6]. In fact, the PAndAS project (Mackey et al. 2010) showed that there are several star clusters within the region Miki et al. (Paper I) proposed for the possible location of the wandering BH. We propose that one of those clusters is the trailing star cluster that has survived against tidal destruction by M31. Such remnant star clusters are likely more metal-enriched than normal globular clusters (as is expected for stars surrounding recoiled BHs; Merritt et al. 2009), since they consist of stars born in the deep gravitational potential of the colliding galaxies. If one obtains an indication of metal richness via red color and/or spectral features/indices, then such star clusters are good candidates for remnant clusters with massive BHs inside.

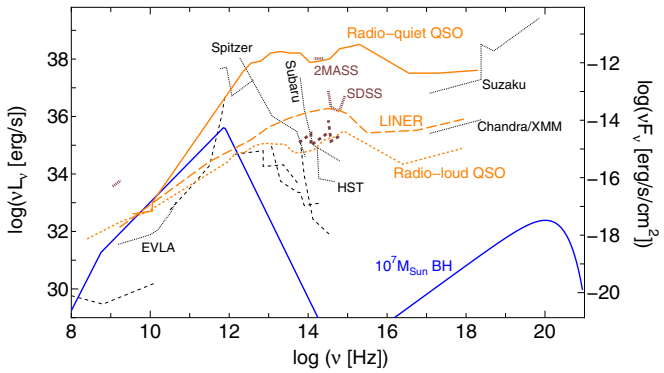

Figure 3. Comparison of the spectral energy distributions between our target (blue solid line for a $10^7\,M_\odot$ BH), a radio-loud QSO at $z \sim 3$, a radio-quiet QSO at $z \sim 0.6$ and a LINER at $z \sim 0.02$ (orange dotted, solid, and dashed lines, respectively; Nemmen et al. 2010). The distances are chosen so that they have similar fluxes at 5 GHz. Detection limits are the same as those in Figure 2.

As another example, at the position of HLX-1 of ESO 243-49, there is a near-IR, optical, and ultraviolet counterpart with a brightness typical of a massive globular cluster (Soria et al. 2010; Farrell et al. 2012). This may be another case of a BH wandering outside the galactic center and trailing a star cluster (see also Annibali et al. 2012; Bekki & Chiba 2004).

4. SUMMARY AND DISCUSSIONS

We have investigated the observational signatures of a massive BH and associated star cluster relic from a late stage of galactic merging in the nearby galaxy M31. M31 likely experienced a merging event with a satellite galaxy about 1 Gyr ago, whose remnants are now observed as stellar sub-structures.

Based on the expected position and velocity of the wandering BH that was originally at the center of the satellite galaxy, we have estimated the current gas accretion rate onto the BH via the Hoyle–Lyttleton–Bondi formula. We then calculated the broadband spectrum using the estimated accretion rate adopting an ADAF model. We find that the emission from the accretion flow is well above the sensitivities of the radio facilities currently operating (EVLA and ALMA Cycle 1). Once the full ALMA and the SKA become operational, we will be able to probe the multi-waveband properties. As the spectral energy distributions of radio-loud and radio-quiet active galactic nuclei and LINERs are very different from that of our target (Figure 3), we can discriminate such background sources from the accretion flow in other wavebands, including the IR, optical, and X-ray.

Another potential approach to search for the wandering massive BH is to hunt for the stars that were in the central region of the satellite galaxy and are thus likely to be more metal-enriched than normal globular clusters. The stars trailed by the BH would be easily detected by near-IR and optical wide-field surveys. We propose that one of the star clusters found by the PAndAS project in the area we constrained for the position of the BH, is the star cluster accompanying the wandering BH.

If we indeed detect such a wandering massive BH associated with the galaxy merging event, it will be an important contribution to exploring how the coevolution of BHs and galaxies proceeds. A discovery will imply a new population of BHs; off-center massive BHs in galactic halos. Recoiling BHs, kicked by the gravitational wave emission during a BH–BH merging event, will have a similar broadband spectral distribution and,

[6] http://wishmission.org

thus, a similar radio detectability. Moreover, such objects will enable us to image the accretion flow around a BH (Luminet 1979; Fukue & Yokoyama 1988), which is practically very difficult for central BHs due to interstellar scattering in the centers of galaxies (Doeleman et al. 2001).

We are grateful to the anonymous referee for detailed comments, and N. Nakai, M. Saito, I. Iwata, and K. Ebisawa for useful discussions, and to Alex Wagner for a careful reading of the manuscript. This work was supported in part by the FIRST project based on Grants-in-Aid for Specially Promoted Research by MEXT (16002003) and Grants-in-Aid for Scientific Research (S) by JSPS (20224002), (A) by JSPS (21244013), and (C) by JSPS (25400222).

REFERENCES

Annibali, F., Tosi, M., Aloisi, A., van der Marel, R. P., & Martinez-Delgado, D. 2012, ApJL, 745, L1
Barth, A. J., Greene, J. E., & Ho, L. C. 2005, ApJL, 619, L151
Bekki, K., & Chiba, M. 2004, A&A, 417, 437
Bellovary, J. M., Governato, F., Quinn, T. R., et al. 2010, ApJL, 721, L148
Bondi, H., & Hoyle, F. 1944, MNRAS, 104, 273
Boroson, T. A., & Lauer, T. R. 2009, Natur, 458, 53
Bower, G., Wright, M. C. H., Falcke, H., & Backer, D. C. 2003, ApJ, 588, 331
Bullock, J. S., & Johnston, K. V. 2005, ApJ, 635, 931
Chiba, M., Minezaki, T., Kashikawa, N., Kataza, H., & Inoue, K. T. 2005, ApJ, 627, 53
Doeleman, S. S., Shen, Z.-Q., Rogers, A. E. E., et al. 2001, AJ, 121, 2610
Fardal, M. A., Guhathakurta, P., Babul, A., & McConnachie, A. W. 2007, MNRAS, 380, 15
Farrell, S. A., Servillat, M., Pforr, J., et al. 2012, ApJL, 747, L13
Farrell, S. A., Webb, N. A., Barret, D., Godet, O., & Rodrigues, J. M. 2009, Natur, 460, 73
Fioc, M., & Rocca-Volmerange, B. 1997, A&A, 326, 950
Font, A. S., Johnston, K. V., Guhathakurta, P., Majewski, S. R., & Rich, R. M. 2006, AJ, 131, 1436
Fukue, J., & Yokoyama, T. 1988, PASJ, 40, 15
Fukugita, M., Shimasaku, K., & Ichikawa, T. 1995, PASP, 107, 945
Godet, O., Plazolles, B., Kawaguchi, T., et al. 2012, ApJ, 752, 34
Hoyle, F., & Lyttleton, R. A. 1939, PCPS, 34, 405
Ibata, R., Irwin, M., Lewis, G., Ferguson, A. M. N., & Tanvir, N. 2001, Natur, 412, 49
Irwin, M. J., Ferguson, A. M. N., Ibata, R. A., Lewis, G. F., & Tanvir, N. R. 2005, ApJL, 628, L105
Jiang, Y.-F., Greene, J. E., Ho, L. C., Xiao, T., & Barth, A. J. 2011, ApJ, 742, 68
Kauffmann, G., & Haehnelt, M. 2000, MNRAS, 311, 576
Komossa, S., Burwitz, V., Hasinger, G., et al. 2003, ApJL, 582, L15
Kormendy, J., & Richstone, D. 1995, ARA&A, 33, 581
Koss, M., Mushotzky, R., Treister, E., et al. 2011, ApJL, 735, L42
Luminet, J.-P. 1979, A&A, 75, 228
Machida, M., Nakamura, K., & Matsumoto, R. 2004, PASJ, 56, 671
Mackey, A. D., Huxor, A. P., Ferguson, A. M. N., et al. 2010, ApJL, 717, L11
Magorrian, J., Tremaine, S., Richstone, D., et al. 1998, AJ, 115, 2285
Mahadevan, R. 1997, ApJ, 477, 585
Marconi, A., & Hunt, L. K. 2003, ApJL, 589, L21
McConnachie, A. W., Irwin, M. J., Ibata, R. A., et al. 2003, MNRAS, 343, 1335
Merritt, D., Schnittman, D., & Komossa, S. 2009, ApJ, 699, 1690
Miki, Y., Mori, M., Kawaguchi, T., & Saito, Y. 2014, ApJ, 783, 87 (Paper I)
Miyazaki, A., Tsutsumi, T., & Tsuboi, M. 2004, ApJL, 611, L97
Mori, M., & Rich, R. M. 2008, ApJL, 674, L77
Narayan, R., & Yi, I. 1995, ApJ, 452, 710
Nemmen, R. S., Storchi-Bergmann, T., Eracleous, M., & Yuan, F. 2010, in IAU Symp. 267, Co-Evolution of Central Black Holes and Galaxies, ed. B. M. Peterson, R. S. Somerville, & T. Storchi-Bergmann (Cambridge: Cambridge Univ. Press), 313
O'Leary, R. M., & Loeb, A. 2009, MNRAS, 395, 781
Perley, R. A., Chandler, C. J., Butler, B. J., & Wrobel, J. M. 2011, ApJL, 739, L1
Perna, R., Narayan, R., Rybicki, G., Stella, L., & Treves, A. 2003, ApJ, 594, 936
Phillips, J. P. 1999, A&AS, 134, 241
Soria, R., Hau, G. K. T., Graham, A. W., et al. 2010, MNRAS, 405, 870
Strader, J., Chomiuk, L., Maccarone, T. J., Miller-Jones, J. C. A., & Seth, A. C. 2012, Natur, 490, 71
Sudou, H., Iguchi, S., Murata, Y., & Taniguchi, Y. 2003, Sci, 300, 1263
Thornton, C. E., Barth, A. J., Ho, L. C., Rutledge, R. E., & Greene, J. E. 2008, ApJ, 686, 892
Walterbos, R. A. M., Brinks, E., & Shane, W. W. 1985, A&AS, 61, 451
Xiao, T., Barth, A. J., Greene, J. E., et al. 2011, ApJ, 739, 28